diversity

MDPI

Article

Marine Bacterial Communities in the Xisha Islands, South China Sea

Yihui Wang [1,2], Lei Wang [2], Yongliang Liu [2], Shengqi Su [1,*] and Wenjin Hao [3,*]

[1] College of Fisheries, Southwest University, Chongqing 400715, China; yhuiwang@outlook.com
[2] Muping Coastal Environment Research Station, Yantai Institute of Coastal Zone Research, Chinese Academy of Sciences, Yantai 264003, China; lwang@yic.ac.cn (L.W.); ylliu@yic.ac.cn (Y.L.)
[3] School of Life Science, Nantong University, Nantong 226019, China
* Correspondence: sushengqi@swu.edu.cn (S.S.); wjhao@ntu.edu.cn (W.H.)

Abstract: Oligotrophic marine environments are ecological funnels in marine ecosystems and are essential for maintaining the health and balance of the entire marine ecosystem. Bacterial communities are one of the most important biological populations, which can survive in low-nutrient environments and perform a variety of important ecological functions, such as decomposing and absorbing organic waste in the ocean and converting nitrogen from the atmosphere into a usable nitrogen source, thus maintaining the health of marine ecosystems. The bacterioplankton community composition and potential function were analyzed using 16S rRNA gene amplicon sequencing in oligotrophic coral reef sea areas. The diversity of the bacterial community exhibited significant differences between the four studied regions. Proteobacteria (38.58–62.79%) were the most abundant in all sampling sites, followed by Cyanobacteria (15.41–37.28%), Bacteroidota (2.39–6.67%), and Actinobacteriota (0.45–1.83%). Although bacterioplankton communities presented no difference between surface and bottom water regarding community richness and α-diversity, the bacterial community composition presented significant differences between surface and bottom water regarding β-diversity. Alteromonadales, Rhodospirllales, and Chloroplast were identified as the significantly different communities between the surface and bottom (Q value < 0.01). Bacterial community distribution in different regions was mainly affected by pH, dissolved oxygen, and nutrients. Nitrite ammonification, chitinolysis, predatory or exoparasitic, chloroplasts, chemoheterotrophy, aerobic chemoheterotrophy, phototrophic, compound degradation (mostly nutrients and pollutants), nitrogen cycle, fermentation, and intracellular parasitism were the dominant functions in the four regions.

Keywords: oligotrophic oceans; bacterial communities; carbon metabolism; nitrogen cycle

Citation: Wang, Y.; Wang, L.; Liu, Y.; Su, S.; Hao, W. Marine Bacterial Communities in the Xisha Islands, South China Sea. *Diversity* **2023**, *15*, 865. https://doi.org/10.3390/d15070865

Academic Editor: Michael Wink

Received: 16 May 2023
Revised: 7 July 2023
Accepted: 14 July 2023
Published: 18 July 2023

1. Introduction

Prokaryotes represent most of the diversity on the planet and are almost certainly the most diverse component of coral reef communities, playing a critical role in marine primary production and biogeochemical cycles [1]. The abundance and impact of marine microbes on biogeochemical processes depended on the balance between their growth and mortality rates [2,3]. Microbial communities, which inhabit a variety of niches within and surrounding coral reefs, are regulated by both bottom-up (nutrient availability) and top-down (predation and viral infection) effects, as well as environmental characteristics, such as temperature [4,5] and light [6,7] in a changing balance. Seawater microbiomes from inshore reefs were previously investigated in order to predict the environmental disturbances that affected the reefs. The composition of bacteria was found to be significantly affected by temperature in addition to water quality parameters such as total suspended solids, particulate organic carbon, and chlorophyll concentrations [8]. Current evidence from multiple studies worldwide has shown that accumulated environmental stress and the capacity of microbial communities to withstand and respond to various abiotic and biotic conditions structure the microbial community [9]. The response of free-living microbial

lineages in reef systems to changes in seawater nutrient gradients and benthic organism composition has been reported [10]. For instance, microbial communities dominated by heterotrophs show 10 times higher microbial abundance in the atoll of the Line Islands chain, accompanied by the highest levels of coral diseases, nitrogen, and phosphate and the lowest coral coverage, including a large percentage of potential pathogens, with characteristics of the nearshore environments [10]. Higher nutrient availability also enriches microbial metabolic traits related to nutrition, such as the ammonification of nitrate and nitrite [11]. Due to the influence of human activities, such as an increase in nitrogen and phosphate concentrations, the bacterial autotrophic communities have transformed from primitive areas dominated by *Prochlorococcus* to atolls dominated by *Synechococcus* [10].

Most of the global oceans are considered oligotrophic areas, generally characterized by a lack of macronutrients such as C, N, and P [12]. Microorganisms in oligotrophic oceans are important components of marine ecosystems. Studies have shown that Proteobacteria, Cyanobacteria, Bacteroidota, and Actinobacteriota are the main bacterial communities in oligotrophic sea areas such as the Indian Ocean [13,14], the South Pacific [15,16], the Western Pacific [17], the South Atlantic [18], and the Mediterranean [19]. Alphaproteobacteria and Gammaproteobacteria are the most abundant in Proteobacteria, and there are different dominant orders in different sea areas. In general, the dominant orders of Alphaproteobacteria are SAR11 [16,18,20] and Rhodobacterales [21,22], and the dominant orders of Gammaproteobacteria are SAR86 [16,18,20] and Alteromonadales [17]. The utilization of proteorhodopsin-conferred photoheterotrophy by the SAR11 and SAR86 clades can result in an improved ability to uptake nutrients. As a decomposer in marine ecosystems, Rhodobacterales can decompose a variety of organic matter, such as aromatics, hydrocarbons, etc. [23]. Alteromonadales are chemoheterotrophic bacteria, some of which have denitrification functions. *Prochlorococcus* and *Synechococcus* are the most abundant in Cyanobacteria. *Synechococcus* and *Prochlorococcus* belong to photosynthetic bacteria, which fix carbon by absorbing carbon dioxide and then converting it into particulate or dissolved organic carbon through processes such as cell death [24]. Moreover, they adapt to environmental nitrogen deficiency by absorbing dissolved organic nitrogen such as amines, urea, nitrile, and amino acids [13,25–27]. Bacteroidota is mainly composed of Flavobacteriales, which produce extracellular hydrolases to degrade macromolecular organic substances. Meanwhile, Flavobacteriales can also metabolize sulfur-containing substances and participate in the sulfur cycle [28–30].

The South China Sea is the largest sea area in China and one of the largest marginal marine areas in the world, which exchanges water with the western Pacific through the Luzon Strait. The nitrate and phosphate content detected in the euphotic layer of the South China Sea is often lower than the detection threshold, which is considered to be a giant subtropical oligotrophic water body [31–33] The northwestern South China Sea has typical coral reef islands in the tropical sea area. Studies have concentrated on coral symbiotic microorganisms in coral reef waters for a long time. Previous reports have suggested that coral symbiotic microorganisms participate in the C, N, P, and S cycles of coral symbiotic functional bodies [34–38] and also play an important role in coral larval attachment [39] and coral resistance to pathogens [40–42]. The conservation of functions and ecosystem services are crucial for maintaining healthy coral reef systems. However, to date, there has been no published comparative study on the microbes present in this region and their functional role in maintaining diversity and ecosystem stability. Despite the close relationship between coral reefs and unique microbial communities that has been documented elsewhere [43,44], data pertaining to the taxonomic and phylogenetic composition of bacterioplankton and bacteriobenthos are lacking at present. In the present study, we applied 16S rRNA gene amplicon sequencing to analyze the bacterioplankton and reveal the community composition and potential function of bacterioplankton in oligotrophic coral reef sea areas.

2. Materials and Methods

2.1. Sampling and Physico-Chemical Analysis

Seawater for the experiments was collected from 16 long-term monitoring stations (16°21′38.47″~17°04′43.16″ N, 111°29′45.60″~112°20′24.07″ E) located in the Xisha Islands in July and August 2020 (Figure 1). Six 500 mL seawater samples were obtained from each station including three surface samples (depth: 0 m) and three bottom samples. Due to the special geomorphology in the coral reef areas, the bottom samples were collected from different water depths (Table S1). Seawater samples were collected using 5 L Niskin bottles and were pre-filtered through 3 μm pore-size filters (TCTP, 47 mm, Millipore, Darmstadt, Germany) to remove particle-associated bacteria and then filtered using 0.22 μm pore-sized membranes (GTTP, 47 mm, Millipore, Germany). The membranes were treated with liquid nitrogen and frozen at −80 °C for DNA extraction.

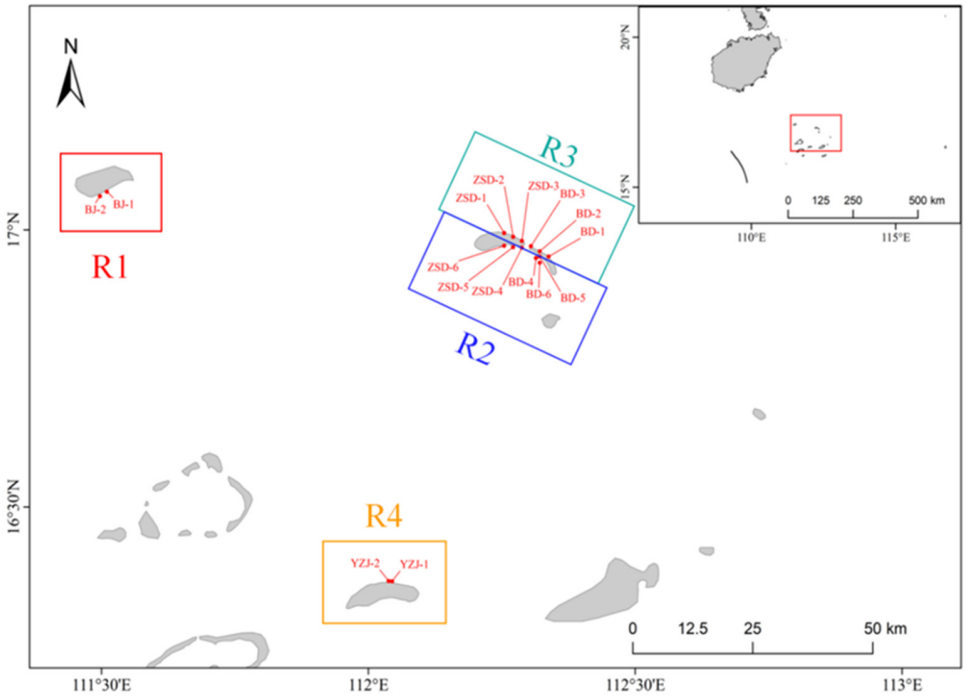

Figure 1. Sampling stations in the Xisha Islands, South China Sea. Note: The 16 sampling sites were divided into 4 groups according to the location of the islands: R1~R4. This map was downloaded from the 1:250,000 National Basic Geographical Database in the National Catalogue Service for Geographic Information (https://www.webmap.cn, accessed on 2 June 2021). BJ: North Atoll, BD: North Island, ZSD: Zhaoshu Island, YZJ: Yuzhuo Atoll.

A YSI 6920 Multiparameter Monitor (USA) was utilized to measure water temperature, salinity, pH, and dissolved oxygen (DO) in situ at the water surface. Samples for nutrient concentration analysis that were collected using 5 L Niskin bottles were filtered through 0.45 μm pore-size filters (CA, 100 mm, Millipore, Germany), after which phosphate (PO_4^{3-}), nitrate (NO_3^-), nitrite (NO_2^-), ammonium (NH_4^+), and silicate (SiO_3^{2-}) concentrations were measured using a QuAAtro Nutrient Salt Automatic Analyzer (SEAL, Hamburg, Germany).

2.2. DNA Extraction, PCR Amplification, and Sequencing

The total DNA in the seawater filter membrane samples was extracted using the PowerWater DNA Isolation Kit (MOBIO, USA), according to the manufacturer's instructions, and monitored for concentration and purity on 1% agarose gel. Sterile water was used to dilute DNA to 1 ng/μL. The variable 3 and 4 regions of 16S rRNA genes were amplified using the specific primers 341F (5′-CCT AYG GGR BGC ASC AG-3′) and 806R (5′-GGA

CTA CNN GGG TAT CTA AT-3′). Overhang sequences as adaptors were linked to the 6 bp barcodes at the 5′ end of each primer. All PCR reactions were carried out using a Phusion High-Fidelity PCR Master Mix (New England Biolabs, Ipswich, MA, USA) with 0.2 μM of each primer and 10 ng template DNA. Thermal cycling consisted of initial denaturation at 98 °C for 1 min, followed by 30 cycles of denaturation at 98 °C for 10 s, annealing at 50 °C for 30 s, and elongation at 72 °C for 30 s and, finally, 72 °C for 5 min. All PCRs were performed in triplicate, including no-template controls in all steps of the process. PCR products were mixed with an equivalent volume of 1× loading buffer (contained SYB green) and electrophoresis on a 2% agarose gel for detection. PCR amplicons with bright bands in each sample were mixed in equal density ratios and purified with a Qiagen Gel Extraction Kit (Qiagen, Hilden, Germany). Following the manufacturer's recommendations, sequencing libraries were generated using the TruSeq® DNA PCR-Free Sample Preparation Kit (Illumina, San Diego, CA, USA), and index codes were added. The library quality was evaluated using a Qubit @ 2.0 fluorometer (Thermo Scientific, Waltham, MA, USA) and the Agilent Bioanalyzer 2100 system. The library sequencing was performed on the Illumina NovaSeq 6000 platform at Novogene Bioinformatics Technology Co., Ltd. (Beijing, China), generating 250 bp paired-end reads. Unfortunately, 4 samples from the BJ2 station, 1 sample from the ZSD6 station, and 3 samples from the YZJ1 station were lost during DNA extraction. A total of 88 membrane samples were amplified and sequenced.

2.3. Amplicon Sequence Analysis

Paired-end reads were matched to samples using unique barcodes and subsequently trimmed by removing the barcodes and primer sequences. FLASH (V1.2.7) [45] was used to merge paired-end reads, and the splicing sequences were called raw reads. Quality filtering was performed on the raw reads using the QIIME (V1.9.1) [46] quality control process under specific filtering conditions, resulting in high-quality clean reads [47]. The reads were compared with the Silva 138 database [48], and chimera sequences were detected using the UCHIME algorithm [49], after which the chimera sequences were removed to obtain effective reads [50].

Sequences with ≥97% similarity were clustered into the same OTUs, and the representative sequence for each OTU was selected for further annotation using Uparse software (v7.0.1001) [51]. The Silva 138 database [48] based on the Mothur algorithm was used for taxonomic annotation. To normalize the OTU abundance information, a standard sequence number was used, corresponding to the sample with the least sequences.

2.4. Statistical Analysis

Both the surface and bottom samples from each station were combined into one sample to analyze for each sampling site in the comparison between the four regions. Four alpha diversity indices (observed OTUs, Chao1, Shannon, and Simpson) for free-living bacterial communities in seawater were calculated with QIIME (V1.7.0), and box plots were visualized with R software (V3.6.2). A Wilcoxon test was used to test significant differences between bacterioplankton communities. Unweighted unifrac distance at the OTU level was used to determine beta diversity for the bacterioplankton communities using non-metric multi-dimensional scaling (nMDS), and visualization was performed using the ggplot2 and vegan packages of R software (v3.6.2). Statistically significant differences in unweighted unifrac distance among the seawater microbiota were set at $p < 0.05$ using an AMOVA test based on the vegan package of R software (V3.6.2). Community compositional changes were evaluated using an analysis of similarity (ANOSIM) and a multi-response permutation procedure (MRPP). A Metastats analysis was performed to identify the species exhibiting significant differences at different levels between the surface and bottom groups. Bacterioplankton community compositions were analyzed at the distinct classification levels and visualized using the barplot function in R software (V3.6.2).

Canonical correspondence analysis (CCA)was conducted to explore the relationships between the bacterioplankton community compositions and environmental variables using

the vegan package of R software (V3.6.2). The main ecological functions of the microbial community were predicted using functional annotation of prokaryotic taxa (FAPROTAX). The cumulative absolute abundances of the OTUs contributing to functional groups were processed using a logarithm with a base of 10 and visualized in a heat map with R software (V 3.6.2). The CCA model was statistically tested using the function ANOVA with 999 permutations. A linear discriminant analysis effect size (LEfSe) [52] was performed to identify the biomarkers among bacterioplankton communities. The alpha value for the Kruskal–Wallis test was set at 0.05, and the linear discriminant analysis (LDA) score threshold for biomarkers was set at 4.

3. Results

3.1. Seawater Physicochemical Parameters across the Xisha Islands

The nutrient parameters for the sixteen sampling sites in the four regions of the Xisha Islands are shown in Figure 2 and Table S2. The physical parameters of seawater, including temperature, pH, salinity, and dissolved oxygen.at the sixteen sampling sites are shown in Table S3. The seawater samples taken from the sixteen sampling sites exhibited temperatures ranging from 30.4 °C to 31.9 °C and pH values ranging from 7.75 to 8.33. The salinity of BD-4 was 33.20, while the salinity range for the other 15 sites was between 34.10 and 34.36. Dissolved oxygen had a gentle fluctuation from site S9 to site 16 (R3 and R4). The phosphate (PO_4^{3-}), nitrate (NO_3^-), nitrite (NO_2^-), ammonium (NH_4^+), and silicate (SiO_3^{2-}) concentrations in all sites ranged from 0.0007 ± 0.000357 to 0.00763 ± 0.00282 mg/L, 0.00551 ± 0.00307 to 0.0319 ± 0.000351 mg/L, 0.00044 ± 0.000212 to 0.00133 ± 0.000102 mg/L, 0.00939 ± 0.00223 to 0.0216 ± 0.00225 mg/L, and 0.0304 ± 0.00567 to 0.0844 ± 0.00384 mg/L, respectively. There were no significant differences in phosphate, nitrite, or ammonium at any station between the surface and bottom water ($p > 0.05$), and all maintained a relatively stable value (Figure 2). Nitrate and silicate in the bottom water were significantly higher than in the surface water ($p < 0.05$), especially in sites S3 (ZSD6), S6 (BD4), S10 (BD2), and S12 (ZSD3).

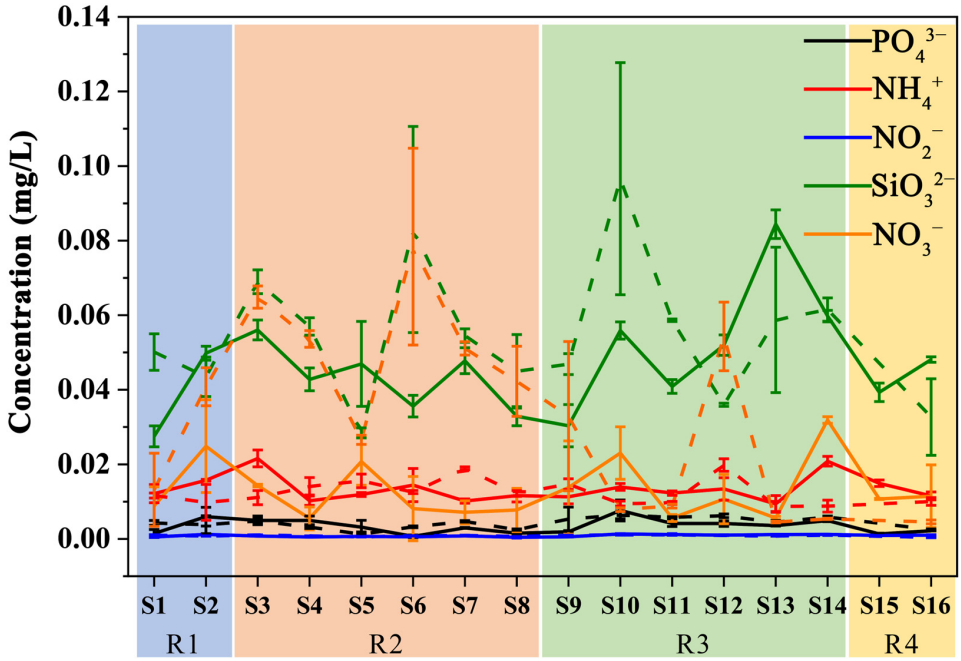

Figure 2. Nutrient parameters for all stations (solid line and dotted line indicate surface and bottom water, respectively). The horizontal axis represents 16 sampling points, and the vertical axis represents the concentration of nutrient parameters (unit: mg/L).

3.2. Diversity of Seawater-Associated Bacterial Communities between the Four Areas in the Xisha Islands

A total of 7,928,966 raw reads were obtained from 88 DNA samples. The median value of raw reads in the surface samples was 91,878, and the median value of raw reads in the bottom samples was 92,118. After tag merging and quality control, a total of 7,786,453 clean tags (98.2% of raw reads) were obtained. The median value of clean tags in the surface samples was 90,606, and the median value of clean tags in the bottom samples was 90,430. The UCHIME algorithm was used to remove potential chimeric tags, resulting in a total of 5,326,150 taxon tags. The tags with ≥97% similarity were grouped into the same operational taxonomic units (OTUs). A total of 75,421 OTUs were observed from all samples, with an average Good's coverage of 99.48 ± 0.00%. Rarefaction analysis and rank abundance curve were utilized to standardize and compare taxon richness between the samples, as well as to assess if the samples were randomly selected (Figure S1). The Chao1 and ACE (abundance-based coverage estimator) indexes, which represent richness, as well as the Shannon–Weaver and Simpson indexes, which indicate diversity, were analyzed, as shown in Figure 3. R4 region (samples collected from Yuzhuo Atoll) presented the highest community richness between the four regions with 1497.42 ± 353.70 and 1587.36 ± 341.06 for Chao1 and ACE, respectively. R4 presented the highest estimated total species and the number of OTUs contained in a community sample. It was significantly different from the R1 and R2 regions ($p = 0.0007$ and 0, Figure 3A,B). The indices of community diversity assessed using the Shannon and Simpson indexes exhibited significant differences between the four regions (Figure 3C,D). The R4 region showed the highest Shannon index (6.09 ± 0.59), followed by R2 (5.28 ± 0.29) and R3 (5.02 ± 0.33), while R1 presented the lowest Shannon index (4.96 ± 1.56). These results indicated that R4 presented high community diversity accompanied by a more uniform species distribution.

The ordination of samples using non-metric multi-dimensional scaling (nMDS), shown in Figure 4, revealed a significant separation of the samples into the four regions, which was supported by the analysis of molecular variance (AMOVA) ($p < 0.001$, Table 1). Moreover, group-to-group and within-group community compositional changes were evaluated using an analysis of similarity (ANOSIM) and the multi-response permutation procedure (MRPP). The results for both methods indicated significant differences ($p < 0.05$) in bacterial communities when comparing the different regions, with greater differences observed between groups than within groups.

3.3. Composition of Seawater-Associated Bacterial Communities between the Four Areas in the Xisha Islands

The top ten phyla with the highest abundance in the sixteen sampling sites are depicted in Figure 5. Proteobacteria were the most abundant phylum in all sampling sites, ranging from 38.58% to 62.79%, followed by Cyanobacteria (15.41–37.28%), Bacteroidota (2.39–6.67%), Actinobacteriota (0.45–1.83%), Firmicutes (0.13–0.87%), and Verrucomicrobiota (0.01–0.51%). The unweighted-pair group method with the arithmetic mean (UPGMA) dendrogram of phylum-level relative abundance, shown in the left panel of Figure 5, was divided into four clusters, each representing one of the regions.

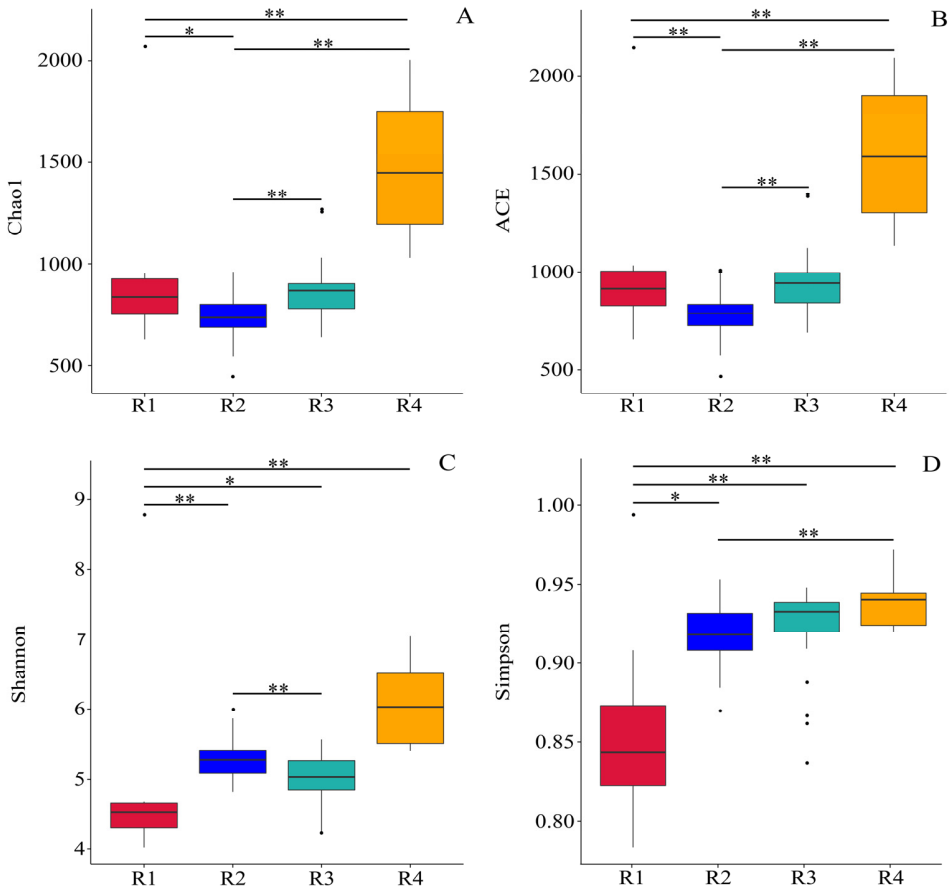

Figure 3. Bacterioplankton community richness and diversity indices for the four regions: (**A**): Chao1, (**B**): ACE, (**C**): Shannon, and (**D**): Simpson. The upper and lower lines in the boxes represent the upper and lower interquartile range (IQR); the middle line represents the median value; and the whiskers represent the maximum and minimum values within 1.5 times IQR. (Significant differences between groups were determined using a Wilcoxon test and are indicated on the top of the graph; *: $p < 0.05$, **: $p < 0.01$).

Table 1. AMOVA pairwise comparisons analysis of bacterial communities between the four groups in the Xisha Islands based on unweighted unifrac dissimilarities. "*" indicated significant difference between the groups.

Vs_Group	SS	df	MS	Fs	*p*-Value
R1–R2	0.862785 (6.85591)	1 (41)	0.862785 (0.167217)	5.15966	<0.001 *
R1–R3	1.07174 (8.51258)	1 (42)	1.07174 (0.202681)	5.28785	<0.001 *
R1–R4	1.00738 (3.29353)	1 (15)	1.00738 (0.219569)	4.58801	<0.001 *
R2–R3	1.01776 (12.7476)	1 (69)	1.01776 (0.184748)	5.50893	<0.001 *
R2–R4	1.24078 (7.52857)	1 (42)	1.24078 (0.179252)	6.92198	<0.001 *
R3–R4	0.757935 (9.18524)	1 (43)	0.757935 (0.21361)	3.54822	<0.001 *
R1–R2–R3–R4	2.98119 (16.0412)	3 (84)	0.993729 (0.190966)	5.20369	<0.001 *

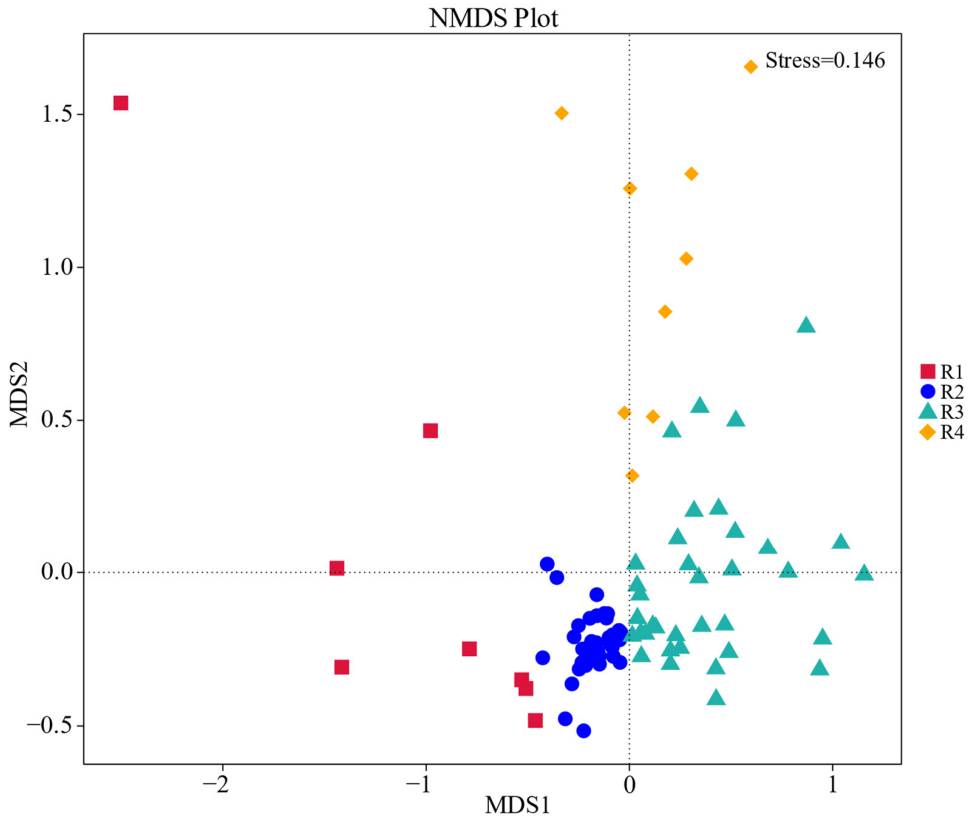

Figure 4. Non-metric multi-dimensional scaling (nMDS) showing the bacterial community between four regions in the Xisha Islands. Each point in the figure represents a sample, and different colors represent different groups.

The distribution of bacterial orders in each sampling region is illustrated in Figure 6, with the relative abundance of the community indicated using colors on the heatmap chart. Colors ranging from deep blue to dark brown correspond to low to high levels of relative abundance, respectively, and the most abundant classes in each site are represented as dark-brown squares within the heatmap chart. Synechococcales, SAR11_clade, Micrococcales, Sphingomonadales, Burkholderiales, Cellvibrionales, Marine Group II, Chitinophagales, Acidobacteriales, and Xanthomonadales were dominant in R1. Rhodospirillales, Bdellovibrionales, SAR86_clade, and Actinomarinales were the predominant orders in R2. R3 harbored high numbers of the abundant communities including Chloroplast, Oceanospirillales, Rhodobacterales, and Flavobacteriales. R4 region had several orders at high abundances, such as Lachnospirales, Bacteroidales, Caulobacterales, Alteromonadales, Rickettsiales, Vibrionales, and Thalassobaculales. The top ten most abundant genera present in each sampling region are shown in Figure S2. The highest numbers of the genus Prochlorococcus_MIT9313 were present in the four regions as follows: R2 (21.86%), R1 (19.8%), R4 (15.81%) and R3 (5.62%). R1 (13.22%) had the highest abundance of Synechococcus, followed by R2 (9.42%), R4(4.8%) and R3(3.81%). R3 had the greatest number of Litoricola, HIMB11, NS5_marine_group, and Shimia, which differed significantly from that in other regions. The abundance of Clade_Ia was higher in R2 (9.32%), R1 (6.92%), and R4 (9.17%), respectively, than in R3 (1.5%).

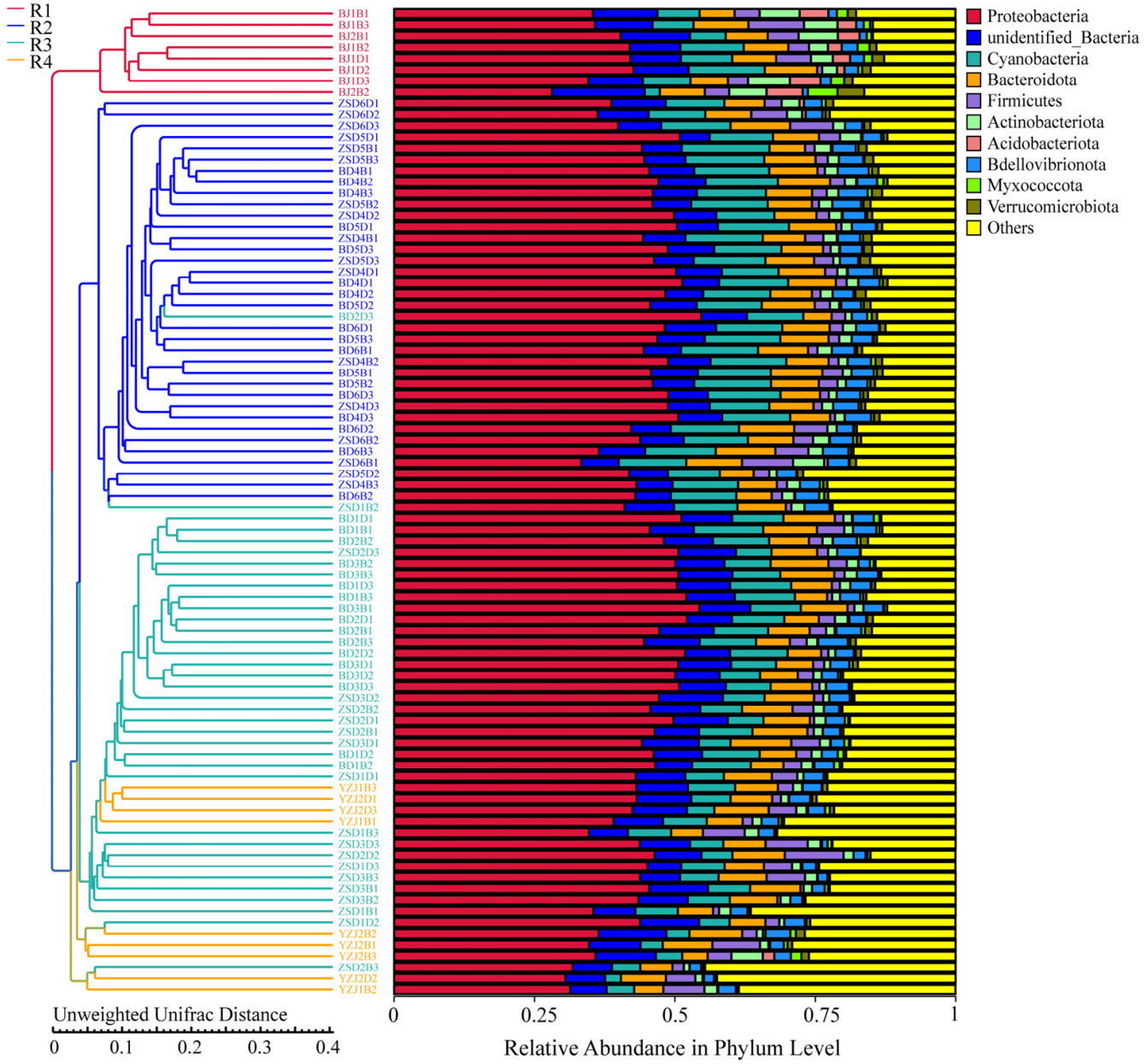

Figure 5. UPGMA dendrogram showing relative abundance at the phylum level at each sampling site. In the left panel, each sample is colored to represent its sampling region. The color in the legend at the upper left indicates the group color for each sample in the clustering tree. The legend at the upper right represents the top 10 species ranked by abundance in the table, with the others classified as "Others".

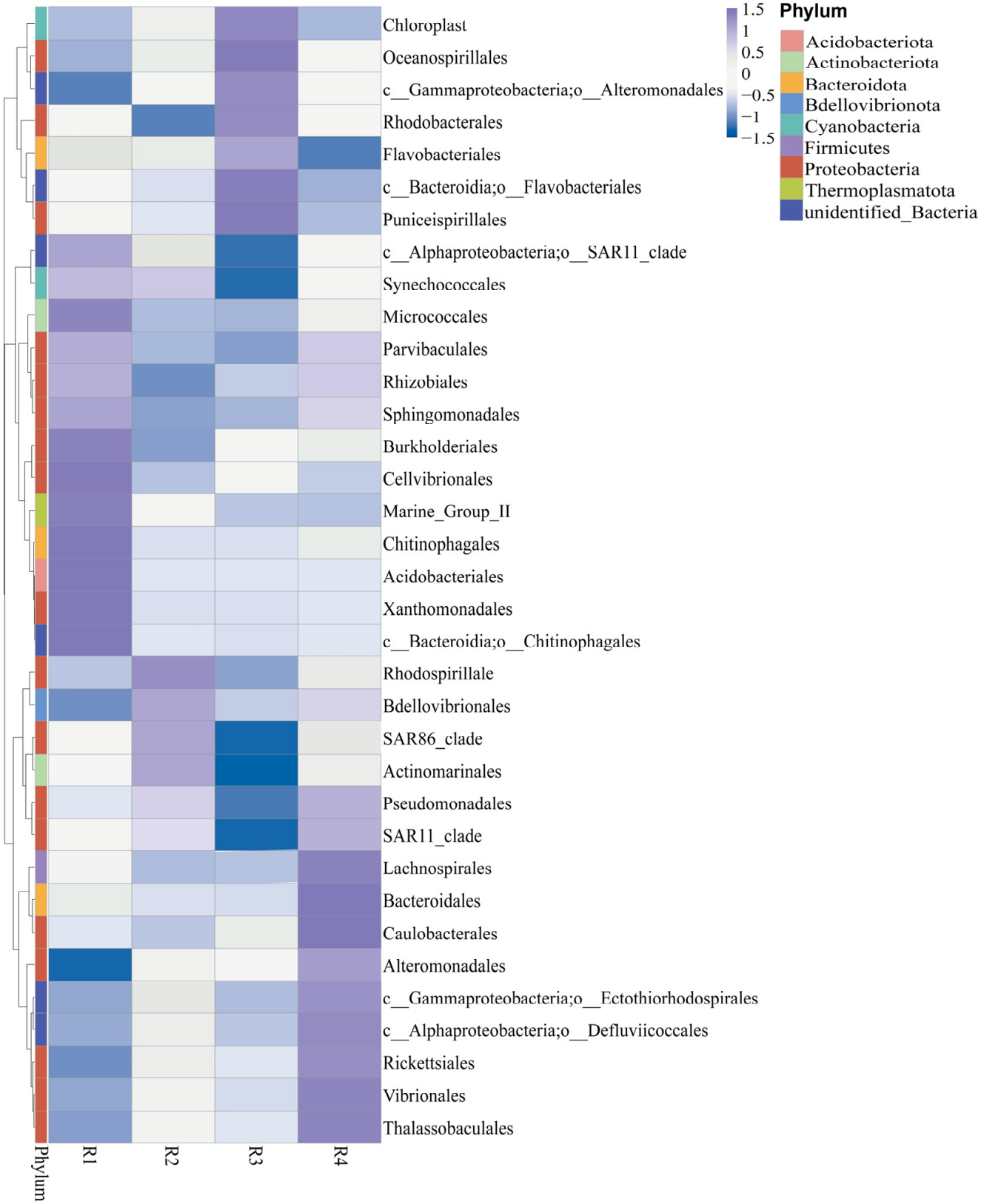

Figure 6. Heat map analysis of bacterial distribution at the order level in the four sampling regions in the Xisha Islands. The color from deep blue to dark brown in the figure corresponds to low to high levels of relative abundance, respectively.

3.4. Diversity and Composition of Bacterioplankton between the Surface and Bottom Water in the Xisha Islands

The bacterioplankton communities presented no difference between the surface and bottom water regarding community richness or diversity (Figure S3). However, the nMDS analysis demonstrated again that the bacterial communities associated with seawater have significant differences between the surface and bottom, according to MRPP (p = 0.025) and ANOSIM (p = 0.029) (Figure S4, Tables S4 and S5). A Metastats analysis was performed to identify the species with significant differences between the surface and bottom groups at different levels (Figure 7). The horizontal axis represents the sample grouping, and the longitudinal axis represents the relative abundance of the corresponding species. The horizontal line represents two groups with significant differences. At the order level, Alteromonadales (belonging to Gammaproteobacteria), Rhodospirllales (belonging to Alphaproteobacteria), and Chloroplast (belonging to Cyanobacteria) exhibited extremely significant differences between the surface and bottom water (Q value < 0.01) (Figure 7A–C). At the genus level, *Alteromonas*, *Ruegeria,* and *Shimia* were the distinct communities between the surface and bottom water (Q value < 0.01) (Figure 7D–F).

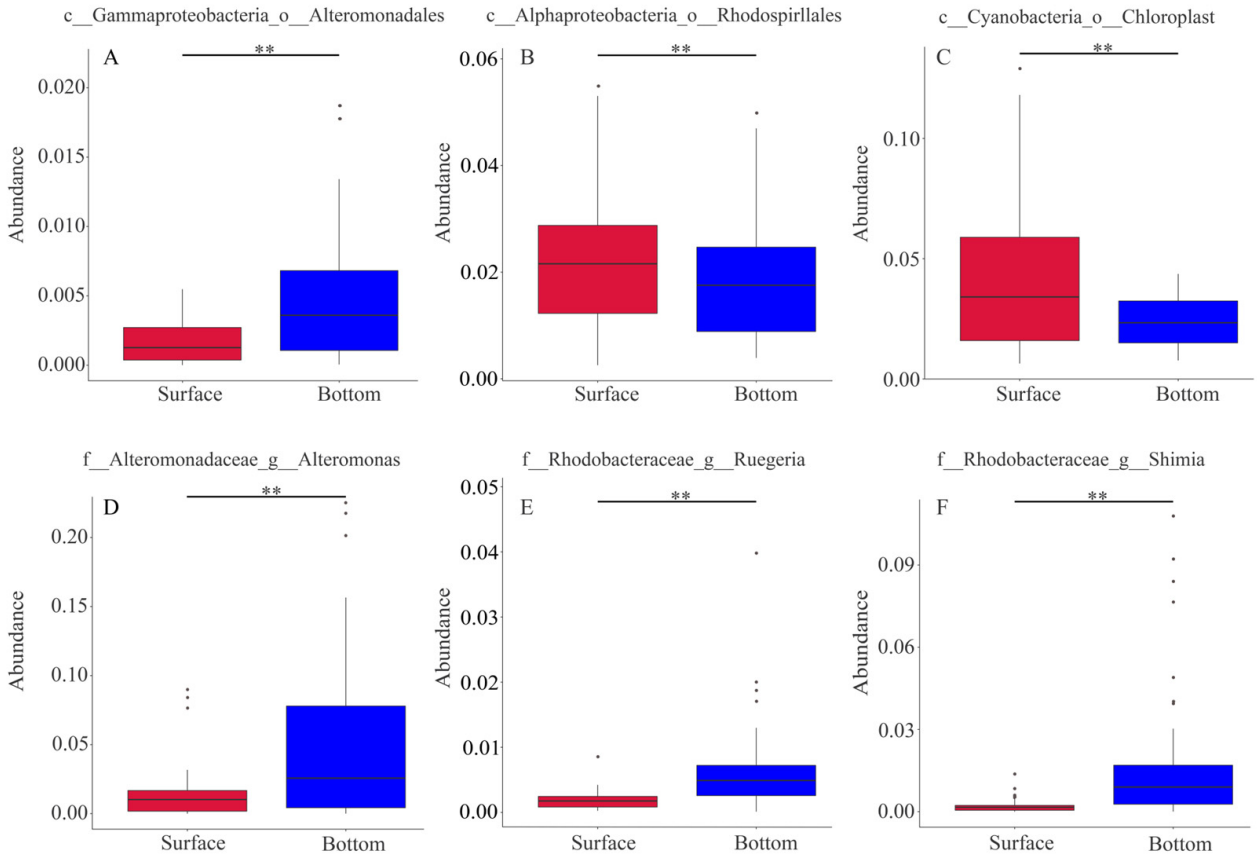

Figure 7. The significantly different species identified between the surface and bottom water from the Xisha Islands at different levels ((**A**–**C**) at the order level; (**D**–**F**) at the genus level). "**" indicates an extremely significant difference between the two groups (Q value < 0.01).

3.5. Distinct Distribution Pattern of Bacterial Communities in Xisha Islands

The bacterioplankton communities in R2 and R3 showed significant differences (AMOVA, p < 0.001). The LEfSe analysis was used to identify significant differences between the two groups (Figure 8). In Figure 8, the vertical axis represents the classification units that exhibited significant differences between groups, and the horizontal axis intuitively displays the log score values of LDA analysis for each classification unit as a bar chart. The classification units are sorted by score value, and the longer the length, the more

significant the differences in the classification unit. The color of the bar indicates the sample grouping with higher abundance. Classes Alphaproteobacteria and Gammaproteobacteria (belonging to phylum Proteobacteria) and Bacteroidia (belonging to phylum Bacteroidota) were significantly more abundant in R3 than in R2. Class Cyanobacteriia (belonging to the phylum Cyanobacteria) was identified as the only biomarker in R2 at the phylum and class levels. The abundance of the orders Flavobacteriales (mainly the genus NS5 marine group), Chloroplast, Puniceispirillales, Rhodobacterales, and Oceanospirillales were high in R3, and three biomarkers (Synechococcales, SAR11 clade, and SAR86 clade) at the order level were identified in R2. The families SAR116 clade, Rhodobacteraceae (mainly genus HIMB11), Alteromonadaceae (mainly genus *Alteromonas*), Litoricolaceae (mainly genus *Litoricola*), and Cryomorphaceae were biomarkers in R3, while Cyanobiaceae (mainly genera *Synechococcus*_CC9902 and *Prochlorococcus*_MIT9313), Clade I (mainly genus Clade Ia), and Clade II were biomarkers in R2.

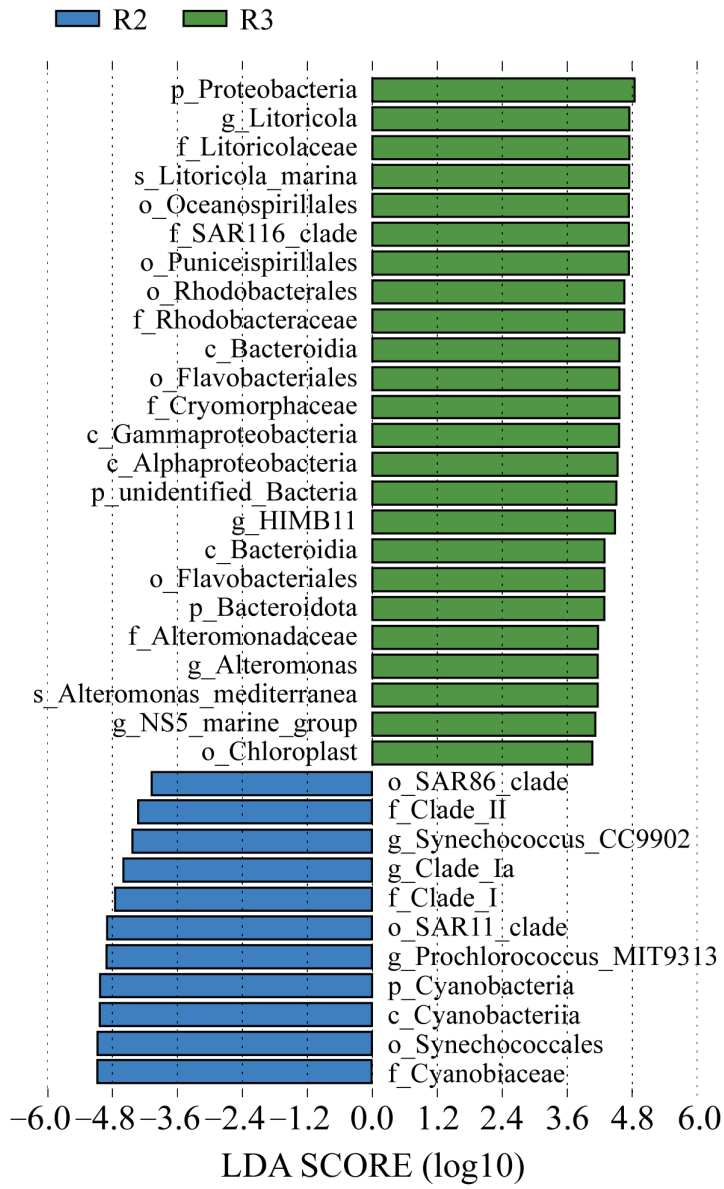

Figure 8. Linear discriminant analysis effect size (Lefse) analysis of bacterioplankton communities in groups R2 and R3. Note: the threshold value for the LDA score was 4.

3.6. Functional Prediction of the 16S Genes Based on FAPROTAX

The heatmap based on the FAPROTAX function prediction indicated that the functional groups that were more abundant in R1 consisted of nitrite ammonification, human diarrhea pathogens, fumarate respiration, ureolysis, and chitinolysis (Figure 9). Human pathogens and predatory or exoparasites had higher abundances in R2 (Figure 9), while Chloroplasts, chemoheterotrophy, and aerobic chemoheterotrophy were the dominant functions in R3 (Figure 9). R4 had 18 significant enrichment function groups, mainly including phototrophic, compound degradation (mostly nutrients and pollutants), the nitrogen cycle, fermentation, and intracellular parasitism (Figure 9).

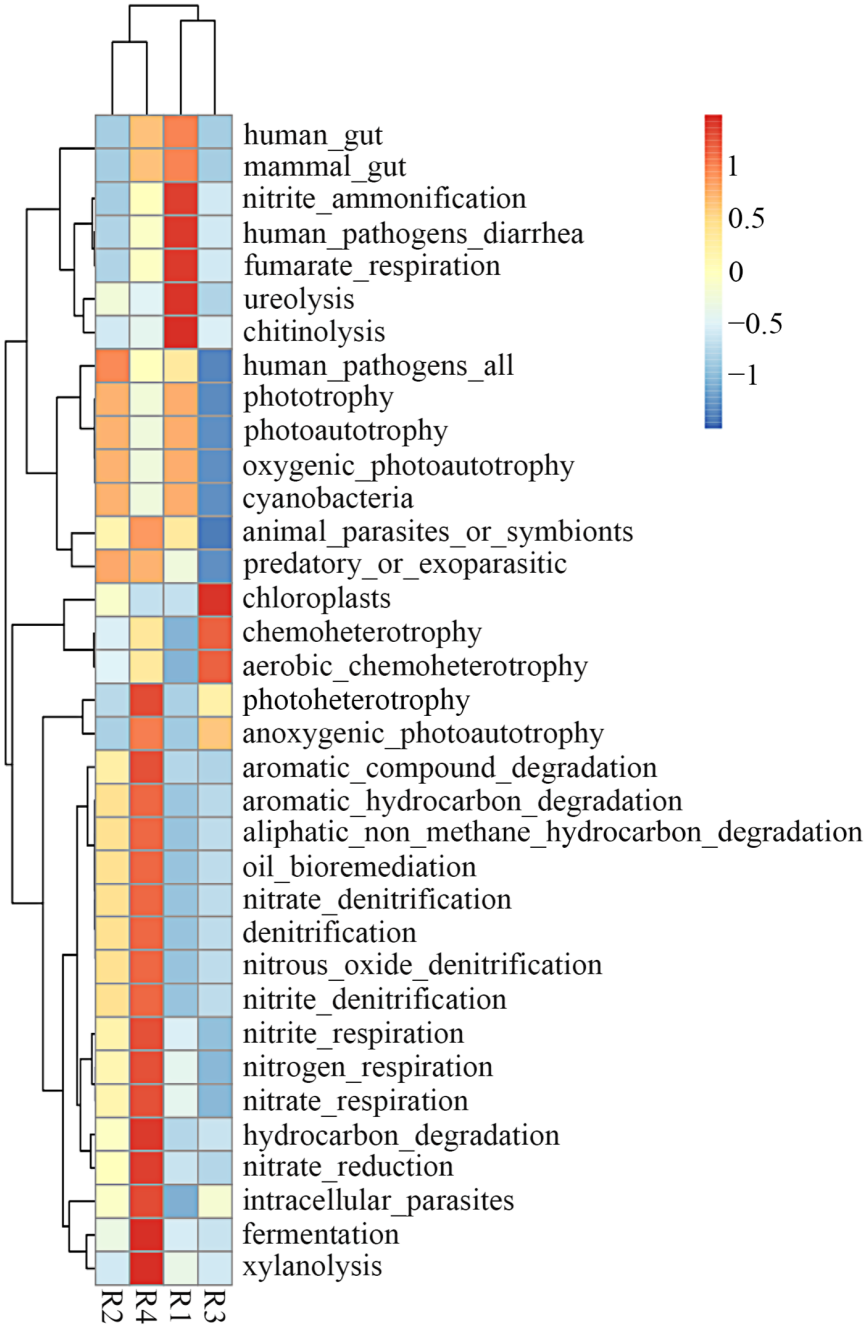

Figure 9. Heatmap showing the abundance of bacterial functional groups analyzed using FAPROTAX between the four sampling areas in the Xisha Islands. The color range from deep blue to dark brown in the figure corresponds to low to high levels of relative abundance, respectively.

3.7. Correlation Analysis between Nutrient Factors and Bacterial Communities

A canonical correspondence analysis (CCA) was performed to investigate the impact of seawater physicochemical parameters on the bacterial communities (Figure 10). In Figure 10, the length of the arrow represents the strength of an environmental factor's impact on community changes, and the longer the arrow, the greater the impact of the environmental factor. The angle between the arrow and the coordinate axis represents the correlation between the environmental factor and the coordinate axis, and the smaller the angle, the higher the correlation. The closer the sample point is to the arrow, the stronger the effect of the environmental factor on the sample. Samples located in the same direction as the arrow indicate a positive correlation between the environmental factor and the change in the species community in the sample, while samples located in the opposite direction of the arrow indicate a negative correlation between the environmental factor and the change in the species community in the sample. Phosphate had the greatest impact on communities in R3. The results showed that nitrite (NO_2^-), phosphate (PO_4^{3-}), and silicate (SiO_3^{2-}) were positively correlated with R3 (Spearman's r = 0.329, p = 0.0005; r = 0.331, p = 0.0005; r = 0.020, p = 0.423), while nitrate (NO_3^-) was positively correlated with R2, and nitrite (NO_2^-), phosphate (PO_4^{3-}), and silicate (SiO_3^{2-}) were negatively correlated with R2, R1, and R4 (r = −0.68, p = 0.04; r = −0.76, p = 0.01).

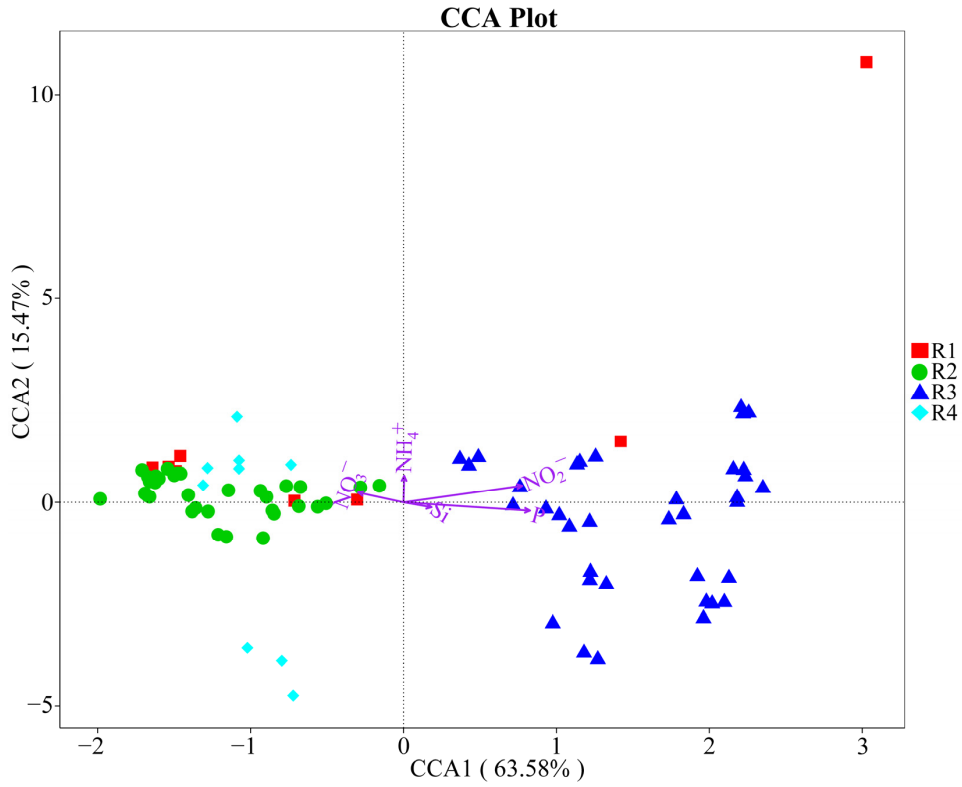

Figure 10. Canonical correspondence analysis (CCA) between the bacterioplankton community compositions and nutrient variables.

4. Discussion

4.1. Relationship between Bacterial Community Composition and Physicochemical Parameters between the Four Areas in the Xisha Islands

The bacterial communities in the four area presented significant differences corresponding to four different indexes (Chao1, ACE, Shannon, and Simpson). The non-metric multi-dimensional scaling (nMDS) analysis showed a significant separation of microbiota communities into different regions in the two-dimensional view. This might be related to environmental factors such as pH, temperature, salinity, dissolved oxygen, and nu-

trients, which were important environmental factors regulating microbial distribution. Proteobacteria, Cyanobacteria, and Bacteroidetes were the most abundant phyla in these four regions. This was consistent with previous findings in oligotrophic waters such as the Indian Ocean [13], the Eastern Mediterranean Sea [53], and the South Pacific Gyre [16], which indicated that Proteobacteria, Cyanobacteria, and Bacteroidetes were the dominant microbial groups in oligotrophic oceans. *Synechococcus*, *Prochlorococcus*, *Litoricola*, HIMB11, and *Alteromonas*, identified here as the major biomarkers, contributed to the significant differences between the bacterioplankton communities in the four studied areas at the order and genus levels. The physical marine environment in the Xisha Islands, which is affected by the Asian monsoon and mesoscale eddies, might explain the observed variation in microbial communities. Furthermore, during July and August, strong southwest winds associated with the East Asian monsoon have a significant impact on the distribution of surface currents and nutrients in the region [54]. Mesoscale eddies contribute to the complex hydrological characteristics of the sea area surrounding the islands [55]. Results from this study showed that the pH range in the different sites was 7.75–8.33, with a large pH fluctuation range. The reason for the significant difference in pH might be due to the biological activity in the coral reef area. Dai et al. [56] showed that biological activity (photosynthesis and respiration) was the main factor affecting pCO_2 in the Xisha coral reef region. Therefore, the lower pH values at certain sites in this study might be due to stronger biological respiration processes in the coral reef area. Meanwhile, the results showed that there were pH-sensitive species, suggesting that pH might be a major factor resulting in different community compositions between the regions. Previous reports suggested that pH affected the composition of bacterial communities, especially some pH-sensitive groups, such as γ-Proteobacteria, Flavobacteriaceae, Rhodobacteraceae, and Campylobacteraceae [57]. Temperature and pH were found to be the main environmental factors regulating the variation in microbial communities between the Red Sea and the Indian Ocean [13]. Here, the dominant genus *Prochlorococcus* was positively correlated with temperature and pH, while *Synechococcus* was negatively correlated with pH. There was little difference in temperature between the different regions, so it was speculated that temperature and salinity had little effect on microbial composition. Meanwhile, except for BD-4, there was a slight variation in salinity between the sampling sites, which might have been caused by ocean currents [58]. Thus, it was speculated that the R2 and R4 regions might be influenced by the same directional ocean current. In contrast, the R1 and R3 regions might be affected by another directional ocean current. Therefore, it was speculated that salinity had little impact on bacterial communities except for BD-4. Considering all sites in the different regions, it was inferred that the difference in salinity might contribute a small part to the variation in bacterial communities between R2 and other regions. Suh et al. [59] discovered that temperature and salinity exerted the most significant influence on the composition of bacterial communities during their study of seasonal dynamic changes in marine microbial communities within the South Sea of Korea. In another study, α-Proteobacteria, γ-Proteobacteria, and Flavobacteria were positively correlated with % NaCl in seawater from the Gulf of Thailand [60]. A study on seawater from Mallorca Island in Spain also revealed a positive correlation between γ-proteobacteria and salinity [61]. Nitrogenase was highly sensitive to the content of dissolved oxygen, where high oxygen concentration significantly inhibited nitrogenase activity, and dissolved oxygen content affected the distribution of nitrogen-fixing microorganisms. Thus, the fluctuation in dissolved oxygen between R3 and R4 might have contributed to the different microbial compositions between R3 and R4.

The correlation analysis between nutrients and the bacterial community showed that NO_2^-, P, and Si were positively correlated with R3 and negatively correlated with R2, R1, and R4, among which NO_2^- and P had a greater impact on R3. NO_3^- was positively correlated with R2. Yuan [62] proposed that the abundance of bacteria in the South China Sea in the summer was limited by carbon and inorganic phosphorus. Jiang [63] also reported that the abundance of planktonic bacteria in Dapeng Bay was positively correlated

with ammonium and phosphate throughout the year. The Mediterranean Sea is similar to the South China Sea, which is also an oligotrophic and nutrient-limited sea area. Here, Lasternas [64] discovered that the abundance and cell viability of planktonic bacteria in the Mediterranean region increased significantly when the phosphorus concentration in seawater increased, indicating that phosphorus was a limiting factor for the growth of plankton in the Mediterranean. Furthermore, nitrogen also affected the bacterioplankton community. The concentrations of nitrate and phosphate were strongly negatively correlated with the relative abundance and growth rates of Roseobacter, Bacteroidetes, and Gammaproteobacteria, while a positive correlation between SAR11 and ammonium was observed [65]. Additionally, Dong [66] demonstrated that nitrogen is a factor in driving changes in bacterial communities, particularly for Rhodothermaceae, Alteromonadaceae, Alcanivoracaceae, Piscirickettsiaceae, and Oceanospirillaceae, whose relative abundance was found to be significantly correlated with nitrate concentration. Cyanobacteria was positively correlated with total phosphorus. In another study, members of β-Proteobacteria, unidentified Proteobacteria, Acidobacteria, and Actinobacteria were positively correlated with total nitrogen, and these results indicated that total nitrogen and total phosphorus were the main factors affecting the bacterial community in the coastal waters from the upper reaches of the Gulf of Thailand [60]. Moreover, the distribution and abundance of benthic organisms were also influenced by nutrients. That study indicated that there was a positive correlation between dissolved inorganic nitrogen (DIN), soluble reactive phosphorus (SRP), particulate organic carbon (POC), and Chl-a and turf algae cover, whereas they were negatively associated with CCA cover and had weak or no correlation with macroalgae cover [67]. Their distribution and abundance might, in turn, affect bacterial communities, for instance, there was a high abundance of *Alteromonas* and *Vibrio* in coral reef microbial communities dominated by algae [11]. Hence, nutrient levels might indirectly impact bacterial communities by influencing benthic organisms. In summary, the distribution of bacterial communities in different regions was mainly affected by pH, dissolved oxygen, and nutrients.

4.2. Composition of Bacterial Communities between the Surface and Bottom Water in the Xisha Islands

There was no difference between the Chao1 and ACE indices or the Shannon and Simpson indices, indicating that there was no difference in bacterial abundance or diversity between surface water and bottom water. Zhang [68] also showed that the Chao1 and Shannon indices for different sites did not change significantly with sampling depth. Further analysis showed that the abundance of Gammaproteobacteria in the surface water was significantly lower than that in the bottom water, while the abundance of Alphaproteobacteria and Cyanobacteria was significantly higher than that in the bottom water.

Currently, global surface seawater is predominantly dominated by Alphaproteobacteria (mainly represented by the SAR11 and SAR116 clusters), as well as Cyanobacteria (particularly *Prochlorococcus*). Previous studies found that Cyanobacteria was the dominant bacteria in the surface water, while Proteobacteria, especially Gammaproteobacteria, was dominant in the deep layers [69]. It was observed that Alphaproteobacteria was mainly distributed in the surface water, and the abundance of Gammaproteobacteria increased with depth in the South China Sea [20,70]. Water depth was an important environmental factor that affects the distribution of microbial communities. Agogue [71] reported that depth and latitude were the two most important variables that explained the diversity of microbial communities in the North Atlantic. The hydrological and hydrochemical parameters of the seawater vary greatly in different water layers. For instance, with an increase in seawater depth, factors such as decreasing light and temperature and increasing available organic matter concentration affect the vertical distribution of microbial communities [72,73].

4.3. Functional Characteristics of Bacterial Communities between the Four Areas in the Xisha Islands

This study further enriched the understanding of the potential functions of bacteria. The FAPROTAX functional prediction revealed that the bacterial community functions in the four regions mainly involved the carbon cycle and nitrogen cycle. This might be related to bacteria, such as *Prochlorococcus*, *Synechococcus*, SAR11, Flavobacteriaceae, etc. *Prochlorococcus* and *Synechococcus*, which had high abundances in the four regions, are known to absorb glucose, leucine, and ATP [74]. Previous studies demonstrated that SAR11, which was abundant in R1 and R2, can also transport amino acids, inorganic ions, and carbohydrates and also plays an important role in the global carbon cycle and has the genetic potential for photosynthesis or phototrophy through protein rhodopsin [21]. In the R3 region, Flavobacteriaceae was the main bacterial group in the marine environment, and this group can degrade a variety of complex organic substances, such as cellulose and chitin, which play an important role in the marine carbon cycle [75–77]. In the R1 region, bacteria of the Sphingomonadales order with a high abundance are known to participate in chemoheterotrophy, including aerobic chemoheterotrophy and chemoheterotrophy. These bacteria can survive in various extreme conditions [78,79] and can utilize a wide range of substrates, such as polycyclic aromatic hydrocarbons (PAHs), polymers, and simple inorganic substances (nitrogen, etc.) [80,81]. Several studies have shown that *Sphingomonas* possesses genes encoding dissimilatory nitrate reductase (nirB) and nitrite reductase (nirB and nirD), which suggests that *Sphingomonas* can possibly further process products of bacterial ammonia oxidation [82,83]. *Alteromonas*, which had higher abundances in R3 and R4, also participates in chemoheterotrophic functions. Some studies also suggested that *Alteromonas* was involved in chitin [84] and petroleum degradation [85]. *Shimia*, which had a certain abundance in R3, was shown to have the potential to degrade petroleum-derived hydrocarbons [85]. The Rhodobacterales bacterium HIMB11, which was a marker in R3, was revealed to be able to synthesize glutamine lipids, replacing membrane glycerophospholipids to accommodate phosphorus limitations [86]. Other studies showed that Vibrionales, which had a high abundance in R4, play a crucial role in the nitrogen cycle, chemoheterotrophy, and fermentation [87]. It is worth mentioning that previous studies had found that *Vibrio* is a prevalent surface and particle colonizer with various chitinases [77,84].

5. Conclusions

The bacterial community composition and potential functions in the oligotrophic ocean were predicted using 16S rRNA gene amplicon sequencing. *Synechococcus*_CC9902, *Prochlorococcus*_MIT9313, *Litoticola*, and *Alteromonas* were the abundant bacterial taxa at the genus level between the four studied regions in the Xisha Islands. The composition of bacterioplankton communities in the surface and bottom layers was significantly different at the order level (mainly Alteromonadales, Rhodospirllales, and Chloroplast) and the genus level (mainly *Alteromonas*, *Ruegeria*, and *Shimia*). pH, dissolved oxygen, and nutrients were important environmental factors regulating bacterial distribution in this region. Between the four regions, the bacterial community in R4 had more diverse functions, mainly including phototrophic, compound degradation (mostly nutrients and pollutants), the nitrogen cycle, fermentation, and intracellular parasitism, while the bacterial community in R2 had the lowest diversity of functions, with higher abundances of human pathogens and predatory or exoparasitic bacteria. Seasonal analysis of the bacterial community, as well as benthic communities, should be considered in future studies to better reveal the functions and interactions between bacterial communities and environmental effects in oligotrophic oceans.

Supplementary Materials: The following supporting information can be downloaded at: https://www.mdpi.com/article/10.3390/d15070865/s1, Figure S1:Rarefaction curves of observed OTU number and rank abundance curve from three samplings of each sampling site analysis; Figure S2:

Stacked Bar plots of bacterial taxa at genus level among four regions in Xisha islands; Figure S3: Bacterioplankton community richness and diversity indices analyzed based on surface and bottom water in Xisha islands, A: Chao1, B: ACE, C: Shannon, D: Simpson; Figure S4: Non-metric multi-dimensional scaling (nMDS) of bacterial community between surface and bottom water in Xisha islands; Table S1: Summary of sampling information; Table S2: Nutrient values of surface water and bottom water among all samples; Table S3: Seawater parameters among all samples; Table S4: MRPP pairwise comparisons analysis of bacterial communities between surface and bottom in Xisha islands based on Bray-Curtis dissimilarities; Table S5: ANOSIM pairwise comparisons analysis of bacterial communities between surface and bottom in Xisha islands based on Bray-Curtis dissimilarities.

Author Contributions: Conceptualization, W.H.; methodology, W.H. and Y.W.; resources, L.W. and Y.L.; writing—original draft preparation, W.H. and Y.W.; writing—review and editing, Y.W. and W.H.; validation, W.H. and S.S.; project administration, W.H.; funding acquisition, W.H. All authors have read and agreed to the published version of this manuscript.

Funding: This research was funded by the National Key Research and Development Program of China (No. 2018YFC1406501) and the National Natural Science Foundation of China (No. 42003064).

Data Availability Statement: The raw sequence data that support the findings of this study were uploaded to NCBI's Sequence Read Archive (SRA) under BioProject accession number PRJNA967315.

Conflicts of Interest: The authors declare no conflict of interest.

References

1. Zinger, L.; Amaral-Zettler, L.A.; Fuhrman, J.A.; Horner-Devine, M.C.; Huse, S.M.; Mark Welch, D.B.; Martiny, J.B.H.; Sogin, M.; Boetius, A.; Ramette, A. Global Patterns of Bacterial Beta-Diversity in Seafloor and Seawater Ecosystems. *PLoS ONE* **2011**, *6*, e24570. [CrossRef] [PubMed]
2. Strom, S.L. Microbial ecology of ocean biogeochemistry: A community perspective. *Science* **2008**, *320*, 1043–1045. [CrossRef] [PubMed]
3. Kirchman, D.L. Growth Rates of Microbes in the Oceans. *Ann. Rev. Mar. Sci.* **2016**, *8*, 285. [CrossRef] [PubMed]
4. Sunagawa, S.; Coelho, L.P.; Chaffron, S.; Kultima, J.R.; Labadie, K.; Salazar, G.; Djahanschiri, B.; Zeller, G.; Mende, D.R.; Alberti, A.; et al. Structure and function of the global ocean microbiome. *Science* **2015**, *348*, 1261359. [CrossRef] [PubMed]
5. Moran, X.A.G.; Gasol, J.M.; Pernice, M.C.; Mangot, J.F.; Massana, R.; Lara, E.; Vaqué, D.; Duarte, C.M. Temperature regulation of marine heterotrophic prokaryotes increases latitudinally as a breach between bottom-up and top-down controls. *Global Chang. Biol.* **2017**, *23*, 3956–3964. [CrossRef]
6. Ruiz-González, C.; Simó, R.; Sommaruga, R.; Josep, M.G. Away from darkness: A review on the effects of solar radiation on heterotrophic bacterioplankton activity. *Front. Microbiol.* **2013**, *4*, 131. [CrossRef]
7. Richert, I.; Dinasquet, J.; Logares, R.; Riemann, L.; Yager, P.L.; Wendeberg, A.; Bertilsson, S. The influence of light and water mass on bacterial population dynamics in the Amundsen Sea Polynya. *Elementa-Sci. Anthrop.* **2015**, *3*, 44. [CrossRef]
8. Glasl, B.; Bourne, D.G.; Frade, P.R.; Thomas, T.; Schaffelke, B.; Webster, N.S. Microbial indicators of environmental perturbations in coral reef ecosystems. *Microbiome* **2019**, *7*, 94. [CrossRef]
9. Martiny, J.B.H.; Bohannan, B.J.M.; Brown, J.H.; Colwell, R.K.; Fuhrman, J.A.; Green, J.L.; Horner-Devine, M.C.; Kane, M.; Krumins, J.A.; Kuske, C.R.; et al. Microbial biogeography: Putting microorganisms on the map. *Nat. Rev. Microbiol.* **2006**, *4*, 102–112. [CrossRef]
10. Dinsdale, E.A.; Pantos, O.; Smriga, S.; Edwards, R.A.; Angly, F.; Wegley, L.; Hatay, M.; Hall, D.; Brown, E.; Haynes, M.; et al. Microbial Ecology of Four Coral Atolls in the Northern Line Islands. *PLoS ONE* **2008**, *3*, e1584. [CrossRef]
11. Kelly, L.W.; Williams, G.J.; Barott, K.L.; Carlson, C.A.; Dinsdale, E.A.; Edwards, R.A.; Haas, A.F.; Haynes, M.; Lim, Y.W.; McDole, T.; et al. Local genomic adaptation of coral reef-associated microbiomes to gradients of natural variability and anthropogenic stressors. *Proc. Natl. Acad. Sci. USA* **2014**, *111*, 10227–10232. [CrossRef]
12. Tyrrell, T. The relative influences of nitrogen and phosphorus on oceanic primary production. *Nature* **1999**, *400*, 525–531. [CrossRef]
13. Wang, Y.Y.; Liao, S.L.; Gai, Y.B.; Liu, G.L.; Jin, T.; Liu, H.; Gram, L.; Strube, M.L.; Fan, G.Y.; Sahu, S.K.; et al. Metagenomic Analysis Reveals Microbial Community Structure and Metabolic Potential for Nitrogen Acquisition in the Oligotrophic Surface Water of the Indian Ocean. *Front. Microbiol.* **2021**, *12*, 518865. [CrossRef] [PubMed]
14. Li, Y. Mechanistic Insights into Microbial Community Structure and Function in South China Sea and Union Glacier and Coexistence of Copiotroph and Oligotroph in The Surface Seawater of India Ocean. Ph.D. Thesis, Shandong University, Jinan, China, 2019. [CrossRef]
15. Qi, Y.; Bingbing, F.; Bingyu, L.; Shi, X.C.; Inagaki, F.; Zhang, X.H. Spatial Variations in Microbial Community Composition in Surface Seawater from the Ultra-Oligotrophic Center to Rim of the South Pacific Gyre. *PLoS ONE* **2013**, *8*, e55148. [CrossRef]

16. West, N.J.; Lepère, C.; Manes, C.O.; Catala, P.; Scanlan, D.J.; Lebaron, P. Distinct Spatial Patterns of SAR11, SAR86, and Actinobacteria Diversity along a Transect in the Ultra-oligotrophic South Pacific Ocean. *Front. Microbiol.* **2016**, *7*, 234. [CrossRef]
17. Bai, J.; Liu, X.S.; Hou, R.; Zhao, Y.G.; Gao, H.W. Community structure and influencing factors of bacterioplankton in the southern South China Sea. *China Environ. Sci.* **2014**, *34*, 2950–2957. [CrossRef]
18. Morris, R.M.; Frazar, C.D.; Carlson, C.A. Basin-scale patterns in the abundance of SAR11 subclades, marine *Actinobacteria* (OM1), members of the *Roseobacter* clade and OCS116 in the South Atlantic. *Environ. Microbiol.* **2012**, *14*, 1133–1144. [CrossRef]
19. Sisma-Ventura, G.; Rahav, E. DOP Stimulates Heterotrophic Bacterial Production in the Oligotrophic Southeastern Mediterranean Coastal Waters. *Front. Microbiol.* **2019**, *10*, 1913. [CrossRef]
20. Li, Y.Y. Microbial Diversity, Nitrogen Utilization Strategy and Environmental Change Response in the Northwest Pacific Ocean and the Basin of the South China Sea. Ph.D. Thesis, Xiamen University, Xiamen, China, 2018.
21. Reintjes, G.; Tegetmeyer, H.E.; Burgisser, M.; Orlić, S.; Tews, I.; Zubkov, M.; Voß, D.; Zielinski, O.; Quast, C.; Glöckner, F.O.; et al. On-Site Analysis of Bacterial Communities of the Ultraoligotrophic South Pacific Gyre. *Appl. Environ. Microbiol.* **2019**, *85*, e00184-19. [CrossRef]
22. Giovannoni, S.J.; Tripp, H.J.; Givan, S.; Podar, M.; Vergin, K.L.; Baptista, D.; Bibbs, L.; Eads, J.; Richardson, T.H.; Noordewier, M.; et al. Genome streamlining in a cosmopolitan oceanic bacterium. *Science* **2005**, *309*, 1242–1245. [CrossRef]
23. Hou, L. Effects of Organic Particles on Microbial Community Structure and Function in the Marine Environment. Ph.D. Thesis, Xiamen University, Xiamen, China, 2019. [CrossRef]
24. Mc Carren, J.; Becker, J.W.; Repeta, D.J.; Shi, Y.M.; Young, C.R.; Malmstrom, R.R.; Chisholm, S.W.; DeLong, E.F. Microbial community transcriptomes reveal microbes and metabolic pathways associated with dissolved organic matter turnover in the sea. *Proc. Natl. Acad. Sci. USA* **2010**, *107*, 16420–16427. [CrossRef] [PubMed]
25. Zubkov, M.V.; Fuchs, B.M.; Tarran, G.A.; Burkill, P.H.; Amann, R. High rate of uptake of organic nitrogen compounds by Prochlorococcus cyanobacteria as a key to their dominance in oligotrophic oceanic waters. *Appl. Environ. Microbiol.* **2003**, *69*, 1299–1304. [CrossRef] [PubMed]
26. García-Fernández, J.M.; de Marsac, N.T.; Diez, J. Streamlined regulation and gene loss as adaptive mechanisms in Prochlorococcus for optimized nitrogen utilization in oligotrophic environments. *Microbiol. Mol. Biol. Rev.* **2004**, *68*, 630–638. [CrossRef] [PubMed]
27. Berthelot, H.; Duhamel, S.; L'Helguen, S.; Maguer, J.; Wang, S.; Cetinić, I.; Cassar, N. NanoSIMS single cell analyses reveal the contrasting nitrogen sources for small phytoplankton. *ISME J.* **2019**, *13*, 651–662. [CrossRef]
28. Howard, E.C.; Sun, S.L.; Reisch, C.R.; del Valle, D.A.; Bürgmann, H.; Kiene, R.P.; Moran, M.A. Changes in dimethylsulfoniopropionate demethylase gene assemblages in response to an induced phytoplankton bloom. *Appl. Environ. Microbiol.* **2011**, *77*, 524–531. [CrossRef]
29. Todd, J.D.; Curson, A.R.J.; Nikolaidou-Katsaraidou, N.; Brearley, C.A.; Watmough, N.J.; Chan, Y.; Page, P.C.B.; Sun, L.; Johnston, A.W.B. Molecular dissection of bacterial acrylate catabolism-unexpected links with dimethylsulfoniopropionate catabolism and dimethyl sulfide production. *Environ. Microbiol.* **2010**, *12*, 327–343. [CrossRef]
30. Raina, J.B.; Tapiolas, D.M.; Foret, S.; Lutz, A.; Abrego, D.; Ceh, J.; Seneca, F.O.; Clode, P.L.; Bourne, D.G.; Willis, B.L.; et al. DMSP biosynthesis by an animal and its role in coral thermal stress response. *Nature* **2013**, *502*, 677–680. [CrossRef]
31. Xiao, P.; Jung, Y.G.; Liu, Y.; Tan, W.H.; Li, W.H.; Li, R.H. Re-evaluation of the diversity and distribution of diazotrophs in the South China Sea by pyrosequencing the nifH gene. *Mar. Freshw. Res.* **2015**, *66*, 681–691. [CrossRef]
32. Wu, C.; Fu, F.X.; Sun, J.; Thangaraj, S.; Pujari, L. Nitrogen fixation by *Trichodesmium* and unicellular diazotrophs in the northern South China Sea and the Kuroshio in summer. *Sci. Rep.* **2018**, *8*, 2415. [CrossRef]
33. Shiozaki, T.; Chen, Y.L.L. Different mechanisms controlling interannual Phytoplankton variation in the South China Sea and the western North Pacific subtropical gyre: A satellite study. *Adv. Space Res.* **2013**, *52*, 668–676. [CrossRef]
34. Lesser, M.P.; Michael, C.H.; Gorbunov, M.Y.; Falkowski, P.G. Discovery of symbiotic nitrogen-fixing Cyanobacteria in corals. *Science* **2004**, *305*, 997–1000. [CrossRef] [PubMed]
35. Lema, K.A.; Willis, B.L.; Bourne, D.G. Corals form characteristic associations with symbiotic nitrogen-fixing bacteria. *Appl. Environ. Microbiol.* **2012**, *78*, 3136. [CrossRef] [PubMed]
36. Kimes, N.E.; Nostrand, J.D.V.; Weil, E.; Zhou, J.Z.; Morris, P.J. Microbial functional structure of *Montastraea faveolata*, an important Caribbean reef -building coral, differs between healthy and yellow-band diseased colonies. *Environ. Microbiol.* **2010**, *12*, 541–556. [CrossRef] [PubMed]
37. Wegley, L.; Edwards, R.A.; Rodriguez-Brito, B.; Liu, H.; Rohwer, F. Metagenomic analysis of the microbial community associated with the coral *Porites astreoides*. *Environ. Microbiol.* **2007**, *9*, 2707–2719. [CrossRef] [PubMed]
38. Zhang, Y.Y.; Ling, J.; Yang, Q.S.; Wen, C.Q.; Yan, Q.Y.; Sun, H.Y.; Van Nostrand, J.D.; Shi, Z.; Zhou, J.Z.; Dong, J.D. The functional gene composition and metabolic potential of coral-associated microbial communities. *Sci. Rep.* **2015**, *5*, 16191. [CrossRef]
39. Sharp, K.H.; Sneed, J.M.; Ritchie, K.B.; Mcdaniel, L.; Paul, V.J. Induction of larval settlement in the reef coral Porites astreoides by a Cultivated Marine Roseobacter Strain. *Biol. Bull.* **2015**, *228*, 98–107. [CrossRef]
40. Ritchie, K.B. Regulation of microbial populations by coral surface mucus and mucus-associated bacteria. *Mar. Ecol. Prog. Ser.* **2006**, *322*, 1–14. [CrossRef]
41. Rypien, K.L.; Ward, J.R.; Azam, F. Antagonistic interactions among coral-associated bacteria. *Environ. Microbiol.* **2009**, *12*, 28–39. [CrossRef]

42. Welsh, R.M.; Zaneveld, J.R.; Rosales, S.M.; Payet, J.P.; Burkepile, D.E.; Thurber, R.V. Bacterial predation in a marine. host-associated microbiome. *ISME J.* **2015**, *10*, 1540–1544. [CrossRef]
43. Frade, P.R.; Glasl, B.; Matthews, S.A.; Mellin, C.; Serrão, E.A.; Wolfe, K.; Mumby, P.J.; Webster, N.S.; Bourne, D.G. Spatial patterns of microbial communities across surface waters of the Great Barrier Reef. *Commun. Biol.* **2020**, *3*, 442. [CrossRef]
44. Silva-Lima, A.W.; Froes, A.M.; Garcia, G.D.; Tonon, L.A.C.; Swings, J.; Cosenza, C.A.N.; Medina, M.; Penn, K.; Thompson, J.R.C.; Thompson, C.; et al. *Mussismilia braziliensis* White Plague Disease Is Characterized by an Affected Coral Immune System and Dysbiosis. *Microb. Ecol.* **2021**, *81*, 795–806. [CrossRef] [PubMed]
45. Magoc, T.; Salzberg, S.L. FLASH: Fast length adjustment of short reads to improve genome assemblies. *Bioinformatics* **2011**, *27*, 2957–2963. [CrossRef] [PubMed]
46. Caporaso, J.G.; Kuczynski, J.; Stombaugh, J.; Bittinger, K.; Bushman, F.D.; Costello, E.K.; Fierer, N.; Peña, A.G.; Goodrich, J.K.; Gordon, J.I.; et al. QIIME allows analysis of high-throughput community sequencing data. *Nat. Methods* **2010**, *7*, 335–336. [CrossRef]
47. Bokulich, N.A.; Subramanian, S.; Faith, J.J.; Gevers, D.; Gordon, J.I.; Knight, R.; Mills, D.A.; Caporaso, J.G. Quality-filtering vastly improves diversity estimates from Illumina amplicon sequencing. *Nat. Methods* **2013**, *10*, 57–59. [CrossRef] [PubMed]
48. Quast, C.; Pruesse, E.; Yilmaz, P.; Gerken, J.; Schweer, T.; Yarza, P.; Peplies, J.; Glöckner, F.O. The SILVA ribosomal RNA gene database project: Improved data processing and web-based tools. *Nucleic Acids Res.* **2013**, *41*, D590-6. [CrossRef]
49. Edgar, R.C.; Haas, B.J.; Clemente, J.C.; Quince, C.; Knight, R. UCHIME improves sensitivity and speed of chimera detection. *Bioinformatics* **2011**, *27*, 2194–2200. [CrossRef]
50. Haas, B.J.; Gevers, D.; Earl, A.M.; Feldgarden, M.; Ward, D.V.; Giannoukos, G.; Ciulla, D.; Tabbaa, D.; Highlander, S.K.; Sodergren, E.; et al. Chimeric 16S rRNA sequence formation and detection in Sanger and 454-pyrosequenced PCR amplicons. *Genome Res.* **2011**, *21*, 494–504. [CrossRef]
51. Edgar, R.C. UPARSE: Highly accurate OTU sequences from microbial amplicon reads. *Nat. Methods* **2013**, *10*, 996–998. [CrossRef]
52. Segata, N.; Izard, J.; Waldron, L.; Gevers, D.; Miropolsky, L.; Garrett, W.S.; Huttenhower, C. Metagenomic biomarker discovery and explanation. *Genome Biol.* **2011**, *12*, R60. [CrossRef]
53. Haber, M.; Rosenberg, D.R.; Lalzar, M.; Burgsdorf, I.; Saurav, K.; Lionheart, R.; Lehahn, Y.; Aharonovich, D.; Gómez-Consarnau, L.; Sher, D.; et al. Spatiotemporal Variation of Microbial Communities in the Ultra-Oligotrophic Eastern Mediterranean Sea. *Front. Microbiol.* **2022**, *13*, 867694. [CrossRef]
54. Cheng, X.R.; Huang, B.Q.; Jian, Z.M.; Zhao, Q.H.; Tian, J.; Li, J.R. Foraminiferal isotopic evidence for monsoonal activity in the South China Sea: A present-LGM comparison. *Mar. Micropaleontol.* **2005**, *54*, 125–139. [CrossRef]
55. Wang, G.H.; Su, J.L.; Chu, P.C. Mesoscale eddies in the South China Sea observed with altimeter data. *Geophys. Res. Lett.* **2003**, *30*, 2121. [CrossRef]
56. Dai, M.H.; Lu, Z.M.; Zhai, W.D.; Chen, B.S.; Cao, Z.M.; Zhou, K.B.; Cai, W.J.; Chen, C.A. Diurnal variations of surface seawater pCO_2 in contrasting coastal environments. *Limnol. Oceanogr.* **2009**, *54*, 735–745. [CrossRef]
57. Krause, E.; Wichels, A.; Giménez, L.; Lunau, M.; Schilhabel, M.B.; Gerdts, G. Small changes in pH have direct effects on marine bacterial community composition: A microcosm approach. *PLoS ONE* **2012**, *7*, e47035. [CrossRef] [PubMed]
58. Ding, Y. Investigation on the Circulation and Coastal Trapped Waves in the Northern South China Sea. Ph.D. Thesis, Ocean University of China, Qingdao, China, 2015.
59. Suh, S.S.; Park, M.; Hwang, J.; Hwang, J.; Kil, E.J.; Jung, S.W.; Lee, S.; Lee, T.K. Seasonal dynamics of marine microbial community in the South Sea of Korea. *PLoS ONE* **2015**, *10*, e0131633. [CrossRef]
60. Nimnoi, P.; Pongsilp, N. Marine bacterial communities in the upper gulf of Thailand assessed by Illumina next-generation sequencing platform. *BMC Biol.* **2020**, *20*, 19. [CrossRef]
61. Héry, M.; Volant, A.; Garing, C.; Luquot, L.; Elbaz Poulichet, F.; Gouze, P. Diversity and geochemical structuring of bacterial communities along a salinity gradient in a carbonate aquifer subject to seawater intrusion. *FEMS Microbiol. Ecol.* **2014**, *90*, 922–934. [CrossRef]
62. Yuan, X.C.; He, L.; Yin, K.D.; Pan, G.; Paul, J.H. Bacterial distribution and nutrient limitation in relation to different water masses in the coastal and northwestern South China Sea in late summer. *Cont. Shelf Res.* **2011**, *31*, 1214–1223. [CrossRef]
63. Jiang, F.J.; Hu, Z.L.; Hu, C.Q. Correlation between spatial-temporal distribution of bacterioplankton and environmental factors in the Dapeng Bay. *J. Trop. Oceanogr.* **2011**, *1*, 96–100. [CrossRef]
64. Lasternas, S.; Agusti, S.; Duarte, C.M. Phyto-and bacterioplankton abundance and viability and their relationship with phosphorus across the Mediterranean Sea. *Aquat. Microb. Ecol.* **2010**, *60*, 175–191. [CrossRef]
65. Teira, E.; Martinez-Garcia, S.; Lonborg, C.; Alvarez-Salgado, X.A. Growth rates of different phylogenetic bacterioplankton groups in a coastal upwelling system. *Environ. Microbiol.* **2009**, *1*, 545–554. [CrossRef] [PubMed]
66. Dong, Z.Y.; Wang, K.; Chen, X.X.; Zhu, J.L.; Hu, C.J.; Zhang, D.M. Temporal dynamics of bacterioplankton communities in response to excessive nitrate loading in oligotrophic coastal water. *Mar. Pollut. Bull.* **2017**, *114*, 656–663. [CrossRef]
67. Liao, Z.H.; Yu, K.F.; Chen, B.; Huang, X.Y.; Qin, Z.J.; Yu, X.P. Spatial distribution of benthic algae in the South China Sea: Responses to gradually changing environmental factors and ecological impacts on coral communities. *Divers. Distrib.* **2021**, *27*, 929–943. [CrossRef]
68. Zhang, H. Diversity, Spatio-Temporal Dynamics, and Biogeographical Modeling of Diazotrophic Community Structures in the northern South China Sea. Master's Thesis, Xiamen University, Xiamen, China, 2010. [CrossRef]

69. Hayedeh, B.; Martin, A.L.; Katsuhiko, M.; Takashi, G. Metagenomic studies of the Red Sea. *Gene* **2016**, *576*, 717–723. [CrossRef]
70. Xu, L. Microbial Communities Structure and in the Northern Slope of South China Sea & Prilimilary Functional Studies of *Kangiella* Strains. Master's Thesis, Shanghai Jiao Tong University, Shanghai, China, 2017. [CrossRef]
71. Agogue, H.; Lamy, D.; Neal, P.R.; Sogin, M.; Herndl, G. Water mass-specificity of bacterial communities in the North Atlantic revealed by massively parallel sequencing. *Mol. Ecol.* **2011**, *20*, 258–274. [CrossRef]
72. Giovannoni, S.J.; Stingl, U. Molecular diversity and ecology of microbial plankton. *Nature* **2005**, *437*, 343–348. [CrossRef]
73. DeLong, E.F.; Preston, C.M.; Mincer, T.; Rich, V.; Hallam, S.J.; Frigaard, N.U.; Martinez, A.; Sullivan, M.B.; Edwards, R.; Brito, B.R.; et al. Community genomics among stratified microbial assemblages in the ocean's interior. *Science* **2006**, *311*, 496–503. [CrossRef] [PubMed]
74. Muñoz-Marín, M.C.; Gómez-Baena, G.; López-Lozano, A.; Moreno-Cabezuelo, J.A.; Díez, J.; García-Fernández, J.M. Mixotrophy in marine picocyanobacteria: Use of organic compounds by *Prochlorococcus* and *Synechococcus*. *ISME J.* **2020**, *14*, 1065–1073. [CrossRef]
75. Suzuki, M.; Nakagawa, Y.; Harayama, S.; Yamamoto, S. Phylogenetic analysis and taxonomic study of marine Cytophaga-like bacteria: Proposal for Tenacibaculum gen. nov. with Tenacibaculum maritimum comb. nov. and Tenacibaculum ovolyticum comb. nov., and description of Tenacibaculum mesophilum sp. nov. and Tenacibaculum amylolyticum sp. nov. *Int. J. Syst. Evol. Micr.* **2001**, *51*, 1639–1652. [CrossRef]
76. Williams, T.J.; Wilkins, D.; Long, E.; Evans, F.; DeMaere, M.Z.; Raftery, M.J.; Cavicchioli, R. The role of planktonic *Flavobacteria* in processing algal organic matter in coastal East Antarctica revealed using metagenomics and metaproteomics. *Environ. Microbiol.* **2013**, *15*, 1302–1317. [CrossRef]
77. Dang, H.; Lovell, C.R. Microbial surface colonization and biofilm development in marine environments. *Microbiol. Mol. Biol. Rev.* **2016**, *80*, 91–138. [CrossRef] [PubMed]
78. Walayat, S.; Malik, A.; Hussain, N.; Lynch, T. Sphingomonas paucimobilis presenting as acute phlebitis: A case report. *IDCases* **2018**, *11*, 6–8. [CrossRef]
79. Menon, R.R.; Kumari, S.; Kumar, P.; Verma, A.; Krishnamurthi, S.; Rameshkumar, N. *Sphingomonas pokkalii* sp. nov., a novel plant associated rhizobacterium isolated from a saline tolerant pokkali rice and its draft genome analysis. *Syst. Appl. Microbiol.* **2019**, *42*, 334–342. [CrossRef] [PubMed]
80. Carmen Garcia, M.; Trujillo, L.A.; Carmona, J.A.; Munoz, J.; Carmen Alfaro, M. Flow, dynamic viscoelastic and creep properties of a biological polymer produced by *Sphingomonas* sp. as affected by concentration. *Int. J. Biol. Macromol.* **2019**, *125*, 1242–1247. [CrossRef] [PubMed]
81. Long, Y.; Yu, Z.H.; Li, Y.Y.; Luo, P.; Jiang, X.; Tian, Y.S.; Ding, X.Q. Ammonia nitrogen and nitrite removal by a heterotrophic *Sphingomonas* sp. strain LPN080 and its potential application in aquaculture. *Aquaculture* **2019**, *500*, 477–484. [CrossRef]
82. Li, Y.; Jing, H.M.; Xia, X.M.; Cheung, S.Y.; Suzuki, K.; Liu, H.B. Metagenomic insights into the microbial community and nutrient cycling in the Western Subarctic Pacific Ocean. *Front. Microbiol.* **2018**, *9*, 623. [CrossRef]
83. Bala, K.; Sharma, P.; Lal, R. Sphingobium quisquiliarum sp. nov., a hexachlorocyclohexane (HCH)-degrading bacterium isolated from an HCH-contaminated soil. *Int. J. Syst. Evol. Micr.* **2010**, *60*, 429–433. [CrossRef]
84. Bakunina, I.; Nedashkovskaya, O.; Balabanova, L.; Zvyagintseva, T.; Rasskasov, V.; Mikhailov, V. Comparative analysis of glycoside hydrolases activities from phylogenetically diverse marine bacteria of the genus *Arenibacter*. *Mar. Drugs* **2013**, *11*, 1977–1998. [CrossRef]
85. Shai, Y.; Rubin-Blum, M.; Angel, D.L.; Sisma-Ventura, G.; Zurel, D.; Astrahan, P.; Rahav, E. Response of oligotrophic coastal microbial populations in the SE Mediterranean Sea to crude oil pollution; lessons from mesocosm studies. *Estuar. Coast. Shelf S.* **2021**, *249*, 107102. [CrossRef]
86. Smith, A.F.; Rihtman, B.; Stirrup, R.; Silvano, E.; Mausz, M.A.; Scanlan, D.J.; Chen, Y. Elucidation of glutamine lipid biosynthesis in marine bacteria reveals its importance under phosphorus deplete growth in *Rhodobacteraceae*. *ISME J.* **2019**, *13*, 39–49. [CrossRef]
87. Peng, S.J.; Hao, W.J.; Li, Y.X.; Wang, L.; Sun, T.T.; Zhao, J.M.; Dong, Z.J. Bacterial communities associated with four blooming scyphozoan jellyfish: Potential species-specific consequences for marine organisms and humans health. *Front. Microbiol.* **2021**, *12*, 647089. [CrossRef] [PubMed]